Published in final edited form as:
AJR Am J Roentgenol. 2011 March ; 196(3): 553–561. doi:10.2214/AJR.10.4580.

Assessment of Chronic Hepatitis and Fibrosis: Comparison of Magnetic Resonance Elastography (MRE) and Diffusion-weighted Imaging (DWI)

Yi Wang[1], **Daniel R. Ganger**[2], **Josh Levitsky**[2], **Laura A. Sternick**[1], **Robert J. McCarthy**[3], **Zongming E. Chen**[4], **Charles W. Fasanati**[1], **Bradley Bolster**[5], **Saurabh Shah**[6], **Sven Zuehlsdorff**[6], **Reed A. Omary**[1], **Richard L. Ehman**[7], and **Frank H. Miller**[1]

[1] Department of Radiology, Northwestern University, Feinberg School of Medicine, 676 N St. Clair, Ste. 800, Chicago, IL 60611

[2] Department of Medicine, Hepatology Division, Northwestern University Feinberg School of Medicine, Chicago, IL

[3] Department of Anesthesiology, Northwestern University Feinberg School of Medicine, Chicago, IL

[4] Department of Pathology, Northwestern University Feinberg School of Medicine, Chicago, IL

[5] Siemens Healthcare, Rochester, MN

[6] Siemens Healthcare, Chicago, IL

[7] Department of Radiology, Mayo Clinic, Rochester, MN

Abstract

Purpose—To compare the utility of magnetic resonance elastography (MRE) and diffusion-weighted imaging (DWI) in characterizing fibrosis and chronic hepatitis in patients with chronic liver diseases.

MATERIALS AND METHODS—Following IRB approval, 76 patients with chronic liver disease underwent abdominal MRI, MRE and DWI. Severities of liver fibrosis and chronic hepatitis were graded by histopathologic analysis according to standard disease-specific classification. The overall predictive ability of MRE and DWI in assessment of fibrosis was compared by constructing a receiver operating characteristic (ROC) curve and calculating the area under the curve (AUC) based on histopathologic analysis.

RESULTS—Using ROC analysis, MRE showed greater capability than DWI in discriminating stage 2 or greater (≥F2), stage 3 or greater (≥F3), cirrhosis (≥F4) shown as significant differences in AUC (P=0.003, P=0.001, P=0.001, respectively). Higher sensitivity/specificity were demonstrated by MRE in predicting fibrosis scores ≥F2 (91%/97%), scores ≥F3 (92%/95%), and scores F4 (95%/87%) compared to DWI (84%/82%, 88%/76%, and 85%/68%). Although MRE had higher ability in identification of liver with fibrosis scores ≥F1 than DWI, a significant difference was not seen (P=0.398). Stiffness values on MRE increased in relation to increasing severity of fibrosis as confirmed by histopathology scores; however, a consistent relationship between apparent diffusion coefficient (ADC) values and stage of fibrosis was not demonstrated. In addition, liver tissue with chronic hepatitis preceding fibrosis may account for mild elevation of liver stiffness.

Address correspondence to F. H. Miller (fmiller@northwestern.edu).

CONCLUSIONS—MRE had greater predictive ability in distinguishing the stages of liver fibrosis compared with DWI.

INTRODUCTION

Hepatic fibrosis is a wound-healing response to multiple types of chronic liver disease and injury [1]. Beyond being a marker of hepatic injury, fibrosis appears to play a direct role in the pathogenesis of cirrhosis, hepatocellular carcinoma and portal venous hypertension, leading to increased morbidity and mortality [2–3]. Effective treatment of chronic liver diseases may result in significant decrease in the severity of hepatic fibrosis, even advanced fibrosis, as seen in hepatitis B and autoimmune hepatitis [4–5]. Accurate determination of the extent of fibrosis is essential in patients with chronic liver disease in order to assess the need for and response to therapy [4–6]. In this regard, liver biopsy has been used as the gold standard for characterization of hepatic fibrosis; however, biopsy has several inherent problems, including sampling error, high cost, morbidity, and low patient acceptance. Biopsy is also too invasive for frequent monitoring to follow treatment response to expensive, and potentially toxic, antifibrotic therapy [7–8]. An equally reliable, reproducible, and noninvasive alternative for the diagnosis and staging of fibrosis would potentially have greater clinical utility.

Recently, magnetic resonance elastography (MRE) has been developed as a noninvasive functional MR imaging method for detecting and staging liver fibrosis. It has been suggested that changes in the mechanical properties of liver tissue such as elasticity and stiffness may correlate with the extent of hepatic fibrosis, effects of chronic hepatitis prior to fibrosis, and/or increased portal venous pressure [9–11]. Liver stiffness among patients with chronic liver disease has been recently evaluated using MRE [12–15]. These studies have shown that increased shear stiffness measured on MRE is associated with increased severity of the fibrotic process. In addition, MRE has a relatively high sensitivity and specificity for predicting the stage of hepatic fibrosis [12–15].

Along with MRE, diffusion-weighted MR imaging (DWI) has been increasingly used to assess liver fibrosis. In theory, DWI measures the random motion of water molecules in biologic tissues, producing representative Apparent Diffusion Coefficient (ADC) values [16]. In prior studies, lower ADC values have been observed in cirrhotic liver compared to normal liver tissue, which may be the result of decreased capillary perfusion and/or restricted diffusion by extracellular fibrosis [17–25]. In addition, it has been shown that ADC values can be used as a predictive marker of moderate and advanced fibrosis [19, 21, 23].

The purpose of our study is to compare the ability of MRE and DWI to detect and characterize chronic hepatitis and liver fibrosis in patients with chronic liver diseases using histopathology as the reference standard.

MATERIAL AND METHODS

Patients

This study was approved by our institutional review board (IRB) and was compliant with the Health Insurance Portability and Accountability Act (HIPAA). Patients were evaluated following written informed consent for acquisition of MRE. Between October 2008 and November 2009, 127 patients with suspected cirrhosis or portal venous hypertension were prospectively evaluated with routine abdominal MRI, MRE and DWI. The inclusion criteria for subjects were as follows: 1) interval time between percutaneous liver biopsy and MR imaging acquisition was less than 1 year; 2) adequate image quality of MRE and DWI was

obtained. Fifty-one patients were excluded in a result of following reasons: lack of histopathological documentation in 42 patients; non-diagnostic exams in 2 patients with hemochromatosis; suboptimal image quality in 2 patients because of the failure to generate a satisfactory mechanical wave through the abdomen. In addition, we excluded patients with other potential causes of elevated stiffness values, including 2 patients with acute rejection of liver transplant, which could cause tissue congestion [11, 26], and 3 patients with portal venous thrombosis, which might contribute to portal hypertension [27]. None of the patients in this study to our knowledge had prior antiviral therapy and none had significant ascites. We avoided any potential artifacts on the diffusion weighted images and the MR elastography.

Our final cohort consisted of 76 patients (50 men and 26 women; median age 55 years; range 20 to 74). The etiologies of chronic liver disease were viral hepatitis in 47 patients (chronic hepatitis C in 44 patients, chronic hepatitis B in 2 patients, chronic hepatitis C combined with alcohol abuse in 1 patient), nonalcoholic steatohepatitis (NASH) in 5 patients, nonalcoholic steatosis in 3 patients, autoimmune diseases in 9 (autoimmune hepatitis in 4 patients and primary sclerosing cholangitis in 5), Wilson's disease in 1, cystic fibrosis in 1, heavy alcohol abuse in 1, and nonspecific chronic liver disease in 9 patients.

MR Imaging

A 1.5-T MR system (Magnetom Espree, Siemens Medical Solutions, Inc., Erlangen, Germany) was used for acquisition of routine clinical MR, MRE and DW images. The gradient strength was 33mT/m with a slew rate of 100 T/m/s. All patients were examined in the supine position. Six-element phased array matrix coil (anterior) and 6-elements of a spine matrix coil (posterior) were used for signal reception.

Routine Abdominal MR Imaging—Our anatomical MR protocol consisted of breath-hold axial and coronal T2-weighted half-Fourier acquisition single-shot turbo spin echo (HASTE), axial in and opposed phase chemical shift imaging, breath-hold T2-weighted turbo spin-echo (TSE) with fat suppression and dynamic contrast enhanced T1-fat suppressed gradient echo images. The parameters of HASTE were the following: repetition time (TR) /echo time (TE), 1000/60 msec; flip angle, 160°; matrix, 256×179; slice thickness, 5 mm without gap; rectangular field of view (FOV), 360–400mm and number of signals acquired, one. Transverse breath-hold in and opposed phase T1-weighted images were obtained by following parameters: TR/TE, 150–200/2.3 (opposed phase) - 4.6 (in phase); flip angle, 70°; matrix, 256×179; section thickness, 6 mm; gap, 1 mm; FOV, 360–400mm; and number of signals acquired, one. Unenhanced and dynamic gadolinium-enhanced T1-weighted images were acquired by fat-suppressed gradient echo imaging using shared prepulses (SHARP). The parameters were the following: TR/TE, 120–160/1.9; flip angle, 80°; slice thickness, 6mm; gap, 1.8mm; matrix, 256×179; FOV, 360–400 mm; 23 slices acquired in breath-hold of 20 seconds. Dynamic gadolinium-enhanced MR images were acquired in the arterial phase (scan time based on fluoroscopy-preparation timing sequence), venous phases (45–60 and 90 seconds), and delayed phase with images obtained 2–5 minutes after contrast injection. Gadopentetate dimeglumine (Magnevist; Bayer HealthCare Pharmaceuticals, Berlin, Germany) was administered at a dose of 0.1 mmol/kg, followed by 20 ml saline flush (2ml/sec) with a power injector (Spectris; Medrad Warrendale, PA).

Magnetic Resonance Elastography—A prototype system for MR Elastography developed at the Mayo Clinic (Rochester, United States) was used for these studies. This system consisted of an acoustic driver system, a gradient echo MRE pulse sequence, and special software for data analysis. A 19-cm diameter, 1.5 cm thick cylindic passive driver was placed against the right chest wall over the liver with the center of the driver at the level

of the xiphoid of the sternum. The passive driver was held in place with an abdominal binder. Continuous acoustic vibration at 60 Hz transmitted from an active driver to the passive driver through a flexible vinyl tube was used to produce propagating shear waves in the liver. A test vibration was first applied on the patient to familiarize the patient with the vibration. The propagating shear waves were imaged with a modified phase contrast gradient-echo sequence (MRE sequence) for collection of axial wave images sensitized along the through-plane direction of motion. The parameters of the MRE sequence were as follows: TR/TE, 100/24.2 msec; flip angle, 15°; bandwidth, 260Hz/pixel; imaging frequency, 63.5MHz; acquisition matrix, 256×64; section thickness, 5mm; FOV, 390×390 mm^2. The scanning time of each transaxial slice was 29 seconds with breath-hold. Four different transaxial slices were acquired. One pair of 1.76 G/cm (1.76×10^{-4} T/cm) motion-encoding gradients was synchronized to the passive pneumatic driver by using a trigger provided by the imager. This trigger was varied to obtain four phase-offset images during a cycle. For each imaging plane, the motion-encoding gradients were applied successively in the two directions orthogonal to the vibration direction of the driver. Quantitative images displaying shear stiffness (MR elastograms) were generated by processing the acquired images of propagating shear waves with a previously described direct inversion algorithm [13–15, 28–29].

DW MR Imaging—All DWI were obtained using a spin-echo echo planar imaging (EPI) sequence. Integrated parallel imaging techniques using generalized autocalibrating partially parallel acquisitions (GRAPPA) were used with a twofold acceleration time. The parameters were: TR/TE, 5000/80msec; bandwidth, 1446 Hz/pixel; acquisition matrix, 156×192; section thickness, 6 mm; gap, 1.8mm; FOV, 300–400 mm; partial Fourier factor 6/8; averages, 2; parallel imaging factor of 2; SPAIR fat saturation pulse; twice-refocused spin-echo diffusion weighting to reduce eddy current-induced distortion with b values of 50, 500 and 1000 sec/mm^2. All separate image series were acquired with diffusion weighting in the axial direction using tridirectional diffusion gradients. The total slices of 2D DW images varied based on the length of the liver and generally approximately 30 slices were acquired when performing DW images.

MR Imaging Analyses

MRE and DW Images Analysis—Two radiologists, with 8 years and 18 years of experience in body MR, performed consensus reading of MRE and DW imaging. The radiologists were blinded to the patients' clinical and histopathologic results.

Based on evaluation of conventional MR images, three round- or oval-shaped regions-of-interest (ROIs) of 2–3 centimeters (cm) were placed on the right lobe of liver. Bile ducts and large vessels within the liver, artifacts from motion, including pulsatile motion artifacts from the heart and aorta, areas with poor signal to noise, and the region just below the driver and left lobe of liver were avoided [13–15].

For stiffness measurement using MRE, the ROI's were first visually transposed into the wave images to ensure that they were placed in regions with adequate wave amplitude. The ROI locations were then visually transposed into the quantitative elastogram images and mean stiffness values (in kilopascals) were calculated [13–15]. The overall stiffness value of the heterogeneous liver was calculated by averaging the mean value of shear stiffness on each slice for the patients. We avoided any potential artifacts such as measurements seen just below the acoustic driver.

For ADC values measurement, the ROIs were placed on the ADC maps. Commercially available imaging software (Syngo, release 2004; Siemens Healthcare, Erlangen, Germany) calculated ADC values on ADC map by averaging the signal intensity in three orthogonal

planes for each b value and subsequently calculating the slope of the logarithmic decay curve for signal intensity against b value [30–31]. Three round- or oval-shaped ROIs of 2–3cm were placed in the right lobe of liver. The ROIs were carefully adjusted according to the adjacent anatomical landmarks to ensure that the placement of ROIs was the same as on the MR elasticity map. In addition, artifacts from motion and liver tissue with poor signal noise were carefully avoided. The ADC values measured on different slices of the ADC map were averaged to determine the overall ADC value of the liver.

Reproducibility Studies—To assess reproducibility of MRE and DWI results, five healthy volunteers who had no known liver disease were scanned. Breath-hold T2-weighted turbo spin-echo (TSE) with fat suppression was acquired for all of healthy volunteers. According to the anatomical imaging, MRE and DWI were obtained using same protocol as in the patients. The exams were performed on two separate occasions and blindly evaluated separated by a period of 2 weeks to avoid memory bias [32]. In addition, twenty-five studies with a variety of the different grades of fibrosis were evaluated on two separate occasions separated by over 6 months to assess interobservor reproducibility.

Liver Histopathology—Specimens were obtained from percutaneous liver biopsies. The quality of specimens was verified by an attending pathologist (C.E.Z). The median time between MR imaging and subsequent biopsy was 60 days (range 1 day and 359 days). Standard techniques for H&E and Masson trichrome staining were applied. Histopathology slides were reviewed by an attending pathologist who was blinded to clinical information and MR results in all cases. The quality of specimens was verified by the same attending pathologist. When grading the fibrosis, areas with large portal tracts or subcapsular fibrotic tissues were excluded. All patients in this study had adequate size biopsies. Fibrosis staging was performed using classification systems developed for the specific liver disease etiologies under study. The METAVIR system [33] was used for patients with chronic viral disease and autoimmune hepatitis. In addition, fibrosis staging for patients with nonalcoholic steatohepatitis (NASH) was based on the Brunt system [34] and fibrosis staging associated with cholestatic liver disease was assessed by the Batts and Ludwig system [35]. Liver fibrosis was classified as the following: F0, no fibrosis; F1, mild fibrosis; F2, moderate fibrosis; F3, advanced fibrosis; F4, cirrhosis. Based on the Batts-Ludwig system [35], grades of hepatocellular necroinflammatory activity were scored as: A0, no activity; A1, mild activity; A2, moderate activity; and A3, severe activity.

Statistical Analysis

Liver shear stiffness values and ADC values are reported as median values with interquartile ranges and assessed by nonparametric methods, because distribution showed substantial departure from normality (standardized kurtosis and standardized skewness >2 and significant Shapiro-Wilks test for normality, $P<0.0001$).

The shear stiffness values and ADC values of different groups were compared using the Kruskal-Wallis H test. Pair-wise comparisons for groups with n>1 were performed using the Mann-Whitney U test with Bonferroni correction for multiple comparisons. The correlation of stiffness values and ADC values with stage of fibrosis was analyzed by the nonparametric method of Spearman's rank correlation coefficient.

Based on the METAVIR system [33], Brunt system [34] and Batts and Ludwig system[35], the overall predictive power of liver stiffness values and ADC values for detecting and staging fibrosis was determined by constructing a receiver operating characteristic (ROC) curve of the sensitivity versus 1– specificity and calculating the area under the curve (AUC). Optimal cutoff values were chosen based on the intersection of sensitivity and specificity, as

well as positive and negative predictive values. AUC values for liver MRE stiffness and ADC values for predicting stage of fibrosis were compared for equivalence using non-parametric methods.

To assess reproducibility of readings using DWI and MRE, twenty five randomly selected patients with no fibrosis and variable stages of fibrosis were assessed by rereading the studies after a period of six months to avoid memory bias. Intra-class correlation for ROI measurements of the cases between the two radiologists was measured using pair-wise comparisons with Tukey's studentized range test. A value greater than 0.75 was considered to represent good agreement [32]. In addition, 95% limits of agreement of stiffness and ADC values between the first and second MRE and DW imaging were evaluated using Bland-Altman plots shown as percentage of mean values to estimate the magnitude of change in ADCs that can confidently be detected in a single individual [32].

A $P < 0.05$ was required to reject the null hypothesis. Statistical analysis was performed with the PASW (Predictive Analytics Software, version 17.02; SPSS Inc. Chicago, IL).

RESULTS

Fibrosis Staging and Necroinflammatory Activity Grading

The stages of fibrosis and grades of necroinflammatory activity observed among the 76 subjects on histopathologic analysis are summarized in Table 1. Among the 32 patients who had no fibrosis, 9 patients had no chronic hepatitis and 23 patients had mild to severe necroinflammatory activity. Of the 44 patients with some degree of fibrosis, 12 patients had fibrosis of stage 1 (Fig 1), 6 had fibrosis of stage 2 (Fig 2), 6 had fibrosis of stage 3 (Fig 3), and 20 had cirrhosis (Fig 4).

Reproducibility of Stiffness and ADC Values Measurements—The 95% limits of agreement between stiffness values measured on repeated MRE imaging ranged from 17.0% to 21.1% of mean stiffness values. The 95% limits of agreement between ADC values measured on DW images ranged from 10.2% to 13.0% of mean ADC values. The stiffness and ADC values of healthy volunteers are summarized in Table 2.

In the 25 studies that were individually reviewed by the two observers, excellent agreement between two observers in measurements of stiffness values using MRE was seen with an intra-class correlation of 0.98, and corresponding 95% confidence interval (95% CI, 0.96–0.99). In comparison, good agreement between two observers in measurements of ADC values using DWI was obtained with an intra-class correlation of 0.83 with 95% CI (0.65–0.92).

Liver Stiffness Values with MR Elastography

Liver tissues without fibrosis had lower median shear stiffness (3.16kPa; interquartile range, 2.62 to 3.58) than tissues with any degree of fibrosis (6.37; 4.73 to 8.12; $P<0.0001$). Liver stiffness values increased with the stage of fibrosis and comparisons of stiffness values in each stage of fibrosis are shown in Table 3. A positive linear correlation between shear stiffness values and stage of fibrosis was observed ($\rho=0.866$; $P<0.0001$).

Furthermore, liver parenchyma with chronic hepatitis and without fibrosis (A1-3/F0) had higher median stiffness values (3.32kPa; interquartile range, 3.03 to 4.10) than that of tissue without chronic hepatitis and fibrosis (A0/F0) (2.61; 1.96 to 2.79; $P=0.0031$). Although liver parenchyma with chronic hepatitis and no fibrosis (A1-3/F0) had lower median stiffness compared to tissue with stage 1 fibrosis (3.50; 3.42 to 3.90), a significant difference was not observed ($P=0.2008$). However, liver parenchyma with chronic hepatitis and without

fibrosis (A1-3/F0) had a significantly lower median stiffness value than those of tissues with stage 2 fibrosis (5.68; 4.65 to 5.97; P=0.0014), stage 3 fibrosis (6.79; 6.10 to 8.56; P=0.0003), and cirrhosis (8.06; 7.07 to 9.91; P<0.0001). Comparison of stiffness values among groups is shown in Figure 5.

Liver ADC Values with DW Imaging

A difference in median ADC values was observed between tissues without fibrosis (1.00×10^{-3}mm^2/sec; interquartile range, 0.95 to 1.06) and tissues with any amount of fibrosis (0.90; 0.86 to 0.99; P<0.0001). Comparison of ADC values in each stage of fibrosis is shown in Table 3. Although an inverse correlation between ADCs and stage of fibrosis was observed ($\rho = -0.661$; P<0.0001), median ADC values did not consistently decrease with increasing stages of fibrosis.

Liver tissue with chronic hepatitis and no fibrosis (A1-3/F0) had a lower median ADC value (0.99×10^{-3}mm^2/sec; interquartile range, 0.94 to 1.02) than tissue without fibrosis and without chronic hepatitis (A0/F0) (1.07; 1.01 to 1.17) with a significant difference (P=0.016). Furthermore, liver parenchyma with chronic hepatitis and without fibrosis (A1-3/F0) had a significantly higher median ADC value than those of parenchyma with each stage of fibrosis (A1-3/Fn) (F1: 0.91; 0.88 to 0.99; P=0.039; F2: 0.89; 0.85 to 0.99; P=0.029; F3; 0.88; 0.81 to 0.90; P=0.016; F4; 0.88; 0.84 to 0.91; P=0.012). Comparison of ADC values among groups is shown in Figure 6.

Comparison of MRE and DW Imaging

Using ROC analysis, MRE demonstrated significantly greater ability in predicting fibrosis stage 2 or greater (≥F2) compared to DWI as shown by AUC/sensitivity/specificity of 0.98/91%/97% and 0.86/84%/82%, respectively (P=0.003). A significant difference in AUC was obtained in predicting stage 3 or greater (≥F3) between MRE (0.99) and DWI (0.84) with sensitivity of 92% and 88%, and specificity of 95% and 76%, respectively (P=0.001). In addition, MRE showed greater capability than DWI in discriminating cirrhosis (F4) as shown by AUC/sensitivity/specificity of 0.95/95%/87% and 0.78/85%/68%, respectively, (P=0.001). ROC analysis showed that AUC/sensitivity/specificity for MRE and DWI were 0.92/72%/100% and 0.88/75%/94% in identification of tissue with fibrosis stage 1 or greater (≥F4); however, a significant difference was not seen (P=0.398).

Cut-off values at intersection of sensitivity and specificity for MRE and DWI in detecting and staging fibrosis are summarized in Table 4. Corresponding sensitivity, specificity, positive predictive value and negative predictive value for MRE and DWI are shown in Table 3. MRE had greater capability in discriminating each stage of fibrosis compared to DWI, as demonstrated by ROC analysis (Fig 7a, b, c, d).

DISCUSSION

In this study, the diagnostic performances of MRE and DWI in detection and characterization of hepatitis and fibrosis in patients with various chronic liver diseases were evaluated and compared. We demonstrated that MRE had greater accuracy in assessing the severity of fibrosis compared to DWI, when using histopathology as the gold standard.

MRE showed a combination of high sensitivity, specificity, positive predictive value and negative predictive value in characterizing severity levels of fibrosis. High accuracy is critical because according to the American Association for the Study of Liver Diseases (AASLD), patients can be accepted as candidates for anti-virus treatment only when substantial fibrosis (≥F2) is observed, especially with hepatitis C genotype 1 infection [6]. High accuracy in discrimination of fibrosis with stage 3 or greater is essential because

patients with advanced fibrosis or cirrhosis should be screened for portal hypertension and hepatocellular carcinoma [6]. Consistent with prior studies [12, 15], we found that liver stiffness values measured on MR elastography increased in parallel with the degree of fibrosis. In particular, MRE showed great ability to identify fibrosis stage ≥2 (F2-4) and stage ≥3 (F2-4) with cut-off values of 5.37kPa and 5.97kPa, representing a combination of high sensitivity (91% and 92%) and specificity (97% and 95%). In comparison, Yin et al. reported sensitivity of 86% and 78% and specificity of 85% and 96% with cut-off values of 4.89kPa and 6.47kPa, respectively [15]. Huwart et al. showed similar high sensitivity of 98% and 95% and specificity of 100% and 100% for discrimination although relatively lower cut-off values of 2.5kPa and 3.1kPa were used [12]. The variety of cut-off values obtained by the present study and prior studies may be potentially explained by MR elastography acquired using different scanner manufacturers, case mix, imaging protocols and/or postprocessing procedures.

Compared to MRE, DWI showed more limited ability in distinguishing each stage of fibrosis with lower sensitivity and specificity. ADC values did not significantly decrease with increasing histopathology stage, which was different from MRE where the observed pressures increased with increasing stages of fibrosis. Nonetheless, liver tissues with fibrosis stage 2 or greater (≥F2) and stage 3 or greater could be distinguished by ADC values on DWI showing sensitivity of 84% and 88%, and specificity 82 % and 76% in the present study. Comparable results with sensitivities of 83% and 89%, and specificities of 83% and 80% was demonstrated by Taouli et al in predicting stage 2 or greater (≥F2) and stage 3 or greater fibrosis (≥F3) [19]. As DW images were acquired by different b values and protocols and likely different patient populations, ADC values of cirrhosis were not consistent throughout the literature. Examples include ADC cut offs of $1.41\pm0.07\times10^{-3}mm^2/sec$ by Taouli et al [19]; $0.88\pm0.26\times10^{-3}mm^2/sec$ by Kim et al [25]; and $1.11\pm0.16\times10^{-3}mm^2/sec$ by Girometti et al. [36]. Although there were various ADC values for the diagnosis of cirrhosis, the cirrhotic liver tissues had consistently significantly lower ADC values compared to liver tissues with no fibrosis as seen in the present study and prior studies [19, 22–23, 25]. Prior published studies with DWI showed moderate sensitivity and specificity in distinguishing advanced fibrosis to cirrhosis (F3–4) from lesser degrees of fibrosis. However, considerable overlap in ADC values between tissues with cirrhosis and with no to moderate fibrosis was also observed [19, 23]. Further study is required to evaluate how various ADC values of liver tissue may be influenced by other factors associated with chronic liver diseases besides fibrosis [16, 20, 37].

In addition, detecting the presence of hepatitis is essential in following liver disease progression because of its close association with the progression of fibrosis and evolution to cirrhosis [4]. As suggested by a prior study, chronic hepatitis before the development of fibrosis may account for elevation of liver stiffness [9]. Liver tissues with pathologically proven chronic hepatitis preceding the development of fibrosis showed mild increased stiffness values on MRE in our study compared to tissues lacking chronic hepatitis and fibrosis. However, chronic hepatitis without fibrosis had less of an influence on the mechanical properties of liver tissue than those with moderate fibrosis to cirrhosis, as shown by the significantly lower stiffness measurements on MRE in our study. In a recent clinical study by Arena et al, a significant increase in stiffness values caused by the onset of acute viral hepatitis was observed using transient US elastography [38]. However, variations in liver stiffness caused by inflammation as a result of chronic hepatitis were not analyzed in prior MRE studies. We also found DWI showed lower mean ADC values of inflamed liver tissue compared to liver tissue without hepatitis and fibrosis. This might suggest that the presence of inflammation, in addition to fibrosis, might influence the restriction of water diffusion and cause a decrease in ADC values.

This study has some potential limitations. First, the small sample size of subjects with fibrosis stage 2 and stage 3 may lead to statistical bias although prior reports have had similar small numbers [15, 19]. In addition, the relatively higher portion of patients with cirrhosis may influence the accuracy of DW imaging in staging fibrosis because the potential for perfusion effects will confound the measurement of diffusion. However, the ADC maps used in the present study were created from diffusion-weighted images with longer b values of 50, 500, and 1000 sec/mm^2 and consequently the perfusion component can be minimized. Second, we did not evaluate the influence of steatosis, iron overload, and edema on stiffness and ADC measurements. Third, we included subjects who underwent biopsy within 1 year of MRE (median interval 60 days). The stage of fibrosis may have changed during the period between biopsy and imaging analysis, which could potentially affect our results. Repeated biopsies were not justified on a clinical basis and the assumption was that a maximum of one year was a reasonable time period.

In conclusion, MRE holds promise as a non-invasive imaging procedure in detecting and staging liver fibrosis in patients with chronic liver disease and has the potential to replace liver biopsy in some patients. As fibrosis is believed to be a dynamic and potentially reversible process with successful treatment, MRE can be potentially used as a technique for monitoring response to therapy. Although DWI showed lower discriminatory capability in staging fibrosis compared to MRE, it may be used as an adjunct MR imaging tool to assess for the presence or absence of severe liver fibrosis especially when MR elastography is not available.

References

1. Rockey DC. Hepatic fibrosis, stellate cells, and portal hypertension. Clin Liver Dis. 2006; 10:459–479. vii–viii. [PubMed: 17162223]
2. Bruix J, Boix L, Sala M, Llovet JM. Focus on hepatocellular carcinoma. Cancer Cell. 2004; 5:215–219. [PubMed: 15050913]
3. El-Serag HB. Hepatocellular carcinoma and hepatitis C in the United States. Hepatology. 2002; 36:S74–83. [PubMed: 12407579]
4. Rockey DC, Bissell DM. Noninvasive measures of liver fibrosis. Hepatology. 2006; 43:S113–120. [PubMed: 16447288]
5. Rockey DC. Current and future anti-fibrotic therapies for chronic liver disease. Clin Liver Dis. 2008; 12:939–962. xi. [PubMed: 18984475]
6. Ghany MG, Strader DB, Thomas DL, Seeff LB. Diagnosis, management, and treatment of hepatitis C: an update. Hepatology. 2009; 49:1335–1374. [PubMed: 19330875]
7. Standish RA, Cholongitas E, Dhillon A, Burroughs AK, Dhillon AP. An appraisal of the histopathological assessment of liver fibrosis. Gut. 2006; 55:569–578. [PubMed: 16531536]
8. Bravo AA, Sheth SG, Chopra S. Liver biopsy. N Engl J Med. 2001; 344:495–500. [PubMed: 11172192]
9. Georges PC, Hui JJ, Gombos Z, et al. Increased stiffness of the rat liver precedes matrix deposition: implications for fibrosis. Am J Physiol Gastrointest Liver Physiol. 2007; 293:G1147–1154. [PubMed: 17932231]
10. Liu Z, Bilston L. On the viscoelastic character of liver tissue: experiments and modelling of the linear behaviour. Biorheology. 2000; 37:191–201. [PubMed: 11026939]
11. Carrion JA, Navasa M, Bosch J, Bruguera M, Gilabert R, Forns X. Transient elastography for diagnosis of advanced fibrosis and portal hypertension in patients with hepatitis C recurrence after liver transplantation. Liver Transpl. 2006; 12:1791–1798. [PubMed: 16823833]
12. Huwart L, Sempoux C, Salameh N, et al. Liver fibrosis: noninvasive assessment with MR elastography versus aspartate aminotransferase-to-platelet ratio index. Radiology. 2007; 245:458–466. [PubMed: 17940304]

13. Rouviere O, Yin M, Dresner MA, et al. MR elastography of the liver: preliminary results. Radiology. 2006; 240:440–448. [PubMed: 16864671]
14. Talwalkar JA, Yin M, Fidler JL, Sanderson SO, Kamath PS, Ehman RL. Magnetic resonance imaging of hepatic fibrosis: emerging clinical applications. Hepatology. 2008; 47:332–342. [PubMed: 18161879]
15. Yin M, Talwalkar JA, Glaser KJ, et al. Assessment of hepatic fibrosis with magnetic resonance elastography. Clin Gastroenterol Hepatol. 2007; 5:1207–1213. e1202. [PubMed: 17916548]
16. Le Bihan D, Breton E, Lallemand D, Aubin ML, Vignaud J, Laval-Jeantet M. Separation of diffusion and perfusion in intravoxel incoherent motion MR imaging. Radiology. 1988; 168:497–505. [PubMed: 3393671]
17. Ziol M, Handra-Luca A, Kettaneh A, et al. Noninvasive assessment of liver fibrosis by measurement of stiffness in patients with chronic hepatitis C. Hepatology. 2005; 41:48–54. [PubMed: 15690481]
18. Yamada I, Aung W, Himeno Y, Nakagawa T, Shibuya H. Diffusion coefficients in abdominal organs and hepatic lesions: evaluation with intravoxel incoherent motion echo-planar MR imaging. Radiology. 1999; 210:617–623. [PubMed: 10207458]
19. Taouli B, Tolia AJ, Losada M, et al. Diffusion-weighted MRI for quantification of liver fibrosis: preliminary experience. AJR Am J Roentgenol. 2007; 189:799–806. [PubMed: 17885048]
20. Taouli B, Koh DM. Diffusion-weighted MR imaging of the liver. Radiology. 2010; 254:47–66. [PubMed: 20032142]
21. Taouli B, Chouli M, Martin AJ, Qayyum A, Coakley FV, Vilgrain V. Chronic hepatitis: role of diffusion-weighted imaging and diffusion tensor imaging for the diagnosis of liver fibrosis and inflammation. J Magn Reson Imaging. 2008; 28:89–95. [PubMed: 18581382]
22. Luciani A, Vignaud A, Cavet M, et al. Liver cirrhosis: intravoxel incoherent motion MR imaging--pilot study. Radiology. 2008; 249:891–899. [PubMed: 19011186]
23. Lewin M, Poujol-Robert A, Boelle PY, et al. Diffusion-weighted magnetic resonance imaging for the assessment of fibrosis in chronic hepatitis C. Hepatology. 2007; 46:658–665. [PubMed: 17663420]
24. Koinuma M, Ohashi I, Hanafusa K, Shibuya H. Apparent diffusion coefficient measurements with diffusion-weighted magnetic resonance imaging for evaluation of hepatic fibrosis. J Magn Reson Imaging. 2005; 22:80–85. [PubMed: 15971188]
25. Kim T, Murakami T, Takahashi S, Hori M, Tsuda K, Nakamura H. Diffusion-weighted single-shot echoplanar MR imaging for liver disease. AJR Am J Roentgenol. 1999; 173:393–398. [PubMed: 10430143]
26. Lee HJ, Kim KW, Mun HS, et al. Uncommon causes of hepatic congestion in patients after living donor liver transplantation. AJR Am J Roentgenol. 2009; 193:772–780. [PubMed: 19696292]
27. Vaidya S, Dighe M, Kolokythas O, Dubinsky T. Liver transplantation: vascular complications. Ultrasound Q. 2007; 23:239–253. [PubMed: 18090835]
28. Muthupillai R, Ehman RL. Magnetic resonance elastography. Nat Med. 1996; 2:601–603. [PubMed: 8616724]
29. Venkatesh SK, Yin M, Glockner JF, et al. MR elastography of liver tumors: preliminary results. AJR Am J Roentgenol. 2008; 190:1534–1540. [PubMed: 18492904]
30. Humphries PD, Sebire NJ, Siegel MJ, Olsen OE. Tumors in pediatric patients at diffusion-weighted MR imaging: apparent diffusion coefficient and tumor cellularity. Radiology. 2007; 245:848–854. [PubMed: 17951348]
31. Bruegel M, Holzapfel K, Gaa J, et al. Characterization of focal liver lesions by ADC measurements using a respiratory triggered diffusion-weighted single-shot echo-planar MR imaging technique. Eur Radiol. 2008; 18:477–485. [PubMed: 17960390]
32. Kim SY, Lee SS, Byun JH, et al. Malignant hepatic tumors: short-term reproducibility of apparent diffusion coefficients with breath-hold and respiratory-triggered diffusion-weighted MR imaging. Radiology. 2010; 255:815–823. [PubMed: 20501719]
33. The French METAVIR Cooperative Study Group. Intraobserver and interobserver variations in liver biopsy interpretation in patients with chronic hepatitis C. Hepatology. 1994; 20:15–20. [PubMed: 8020885]

34. Brunt EM, Janney CG, Di Bisceglie AM, Neuschwander-Tetri BA, Bacon BR. Nonalcoholic steatohepatitis: a proposal for grading and staging the histological lesions. Am J Gastroenterol. 1999; 94:2467–2474. [PubMed: 10484010]

35. Batts KP, Ludwig J. Chronic hepatitis. An update on terminology and reporting. Am J Surg Pathol. 1995; 19:1409–1417. [PubMed: 7503362]

36. Girometti R, Furlan A, Esposito G, et al. Relevance of b-values in evaluating liver fibrosis: a study in healthy and cirrhotic subjects using two single-shot spin-echo echo-planar diffusion-weighted sequences. J Magn Reson Imaging. 2008; 28:411–419. [PubMed: 18666139]

37. Gass A, Niendorf T, Hirsch JG. Acute and chronic changes of the apparent diffusion coefficient in neurological disorders--biophysical mechanisms and possible underlying histopathology. J Neurol Sci. 2001; 186 (Suppl 1):S15–23. [PubMed: 11334986]

38. Arena U, Vizzutti F, Corti G, et al. Acute viral hepatitis increases liver stiffness values measured by transient elastography. Hepatology. 2008; 47:380–384. [PubMed: 18095306]

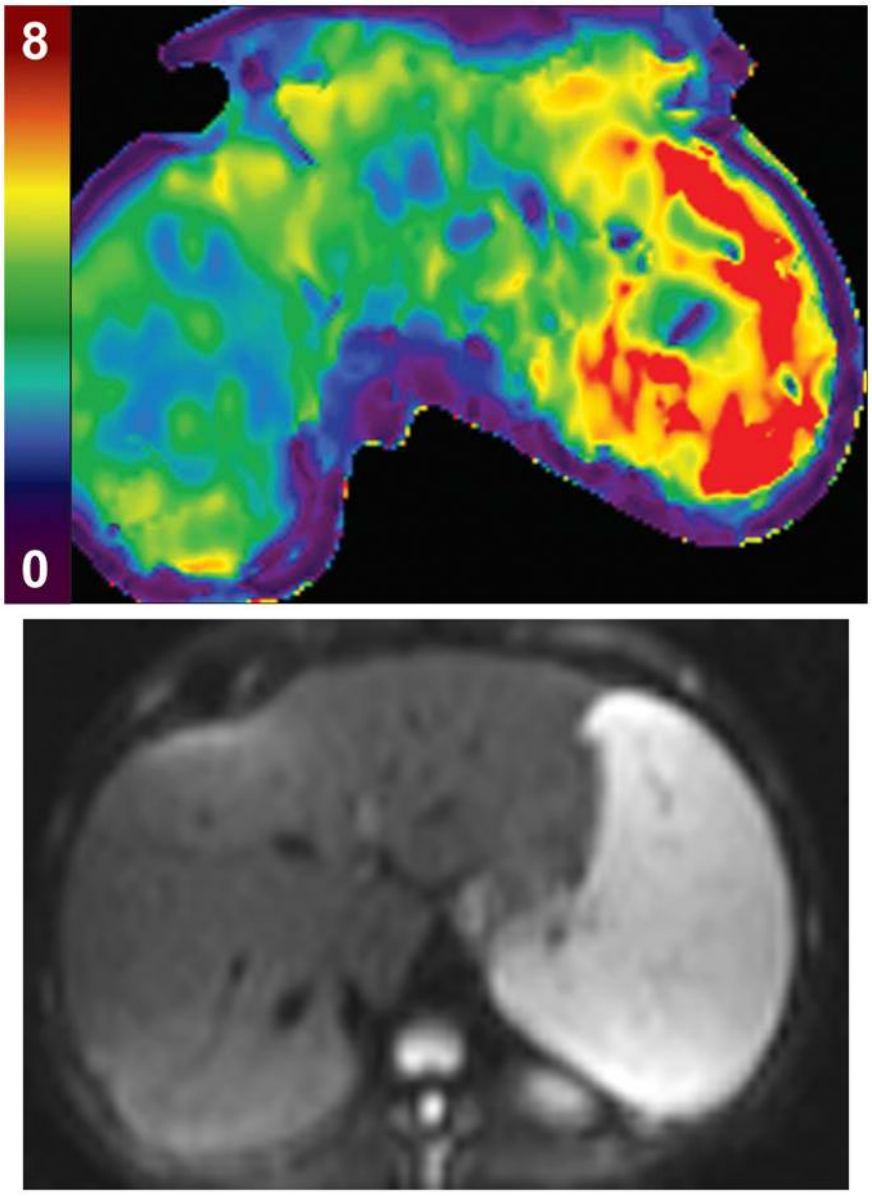

Fig. 1.

20-year-old woman with history of cystic fibrosis. Stage 1 hepatic fibrosis and grade 1 necroinflammatory activity seen at histopathologic analysis following liver biopsy.

A, MR elastogram shows shear stiffness value of 3.45kPa.

B, DWI with b50 sec/mm^2 image had calculated ADC value of 0.99×10^{-3}mm^2/sec.

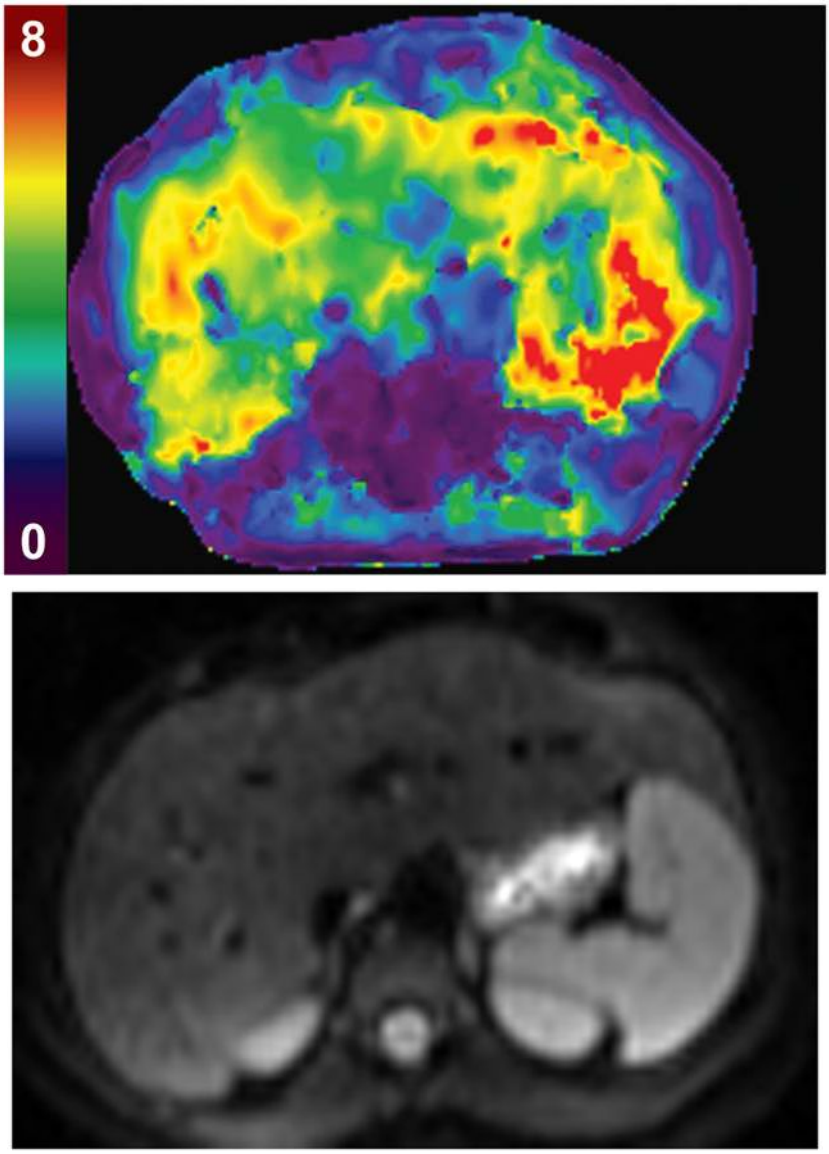

Fig. 2.

47-year-old woman with history of primary sclerosing cholangitis. Stage 2 hepatic fibrosis and grade 2 necroinflammatory activity seen at histopathologic analysis following liver biopsy.

A, MR elastogram shows shear stiffness value of 5.55kPa.

B, DWI with b50 sec/mm^2 image had calculated ADC value of 0.99×10^{-3}mm^2/sec.

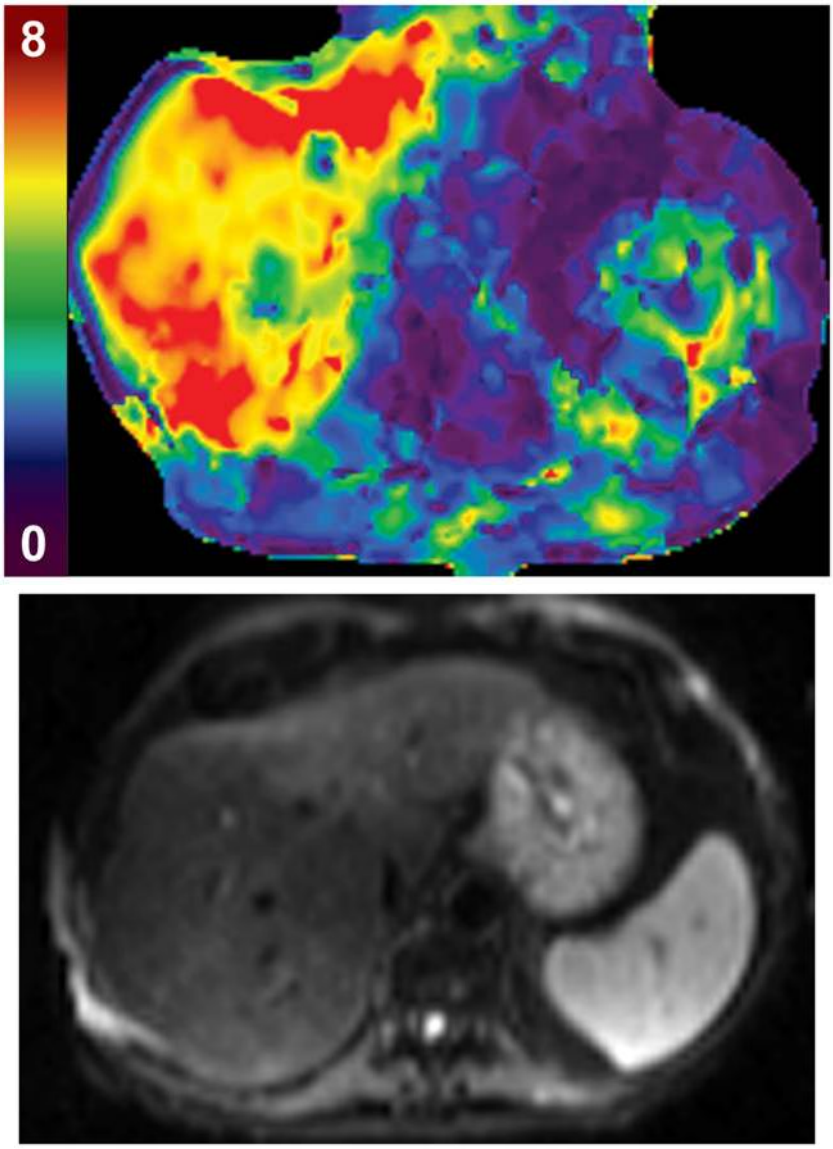

Fig. 3.

56-year-old man with history of heavy alcohol abuse. Stage 3 hepatic fibrosis and grade 1 necroinflammatory activity seen at histopathologic analysis following liver biopsy.

A, MR elastogram shows shear stiffness value of 6.69kPa.

B, DWI with b50 sec/mm^2 image had calculated ADC value of 0.89×10^{-3}mm^2/sec.

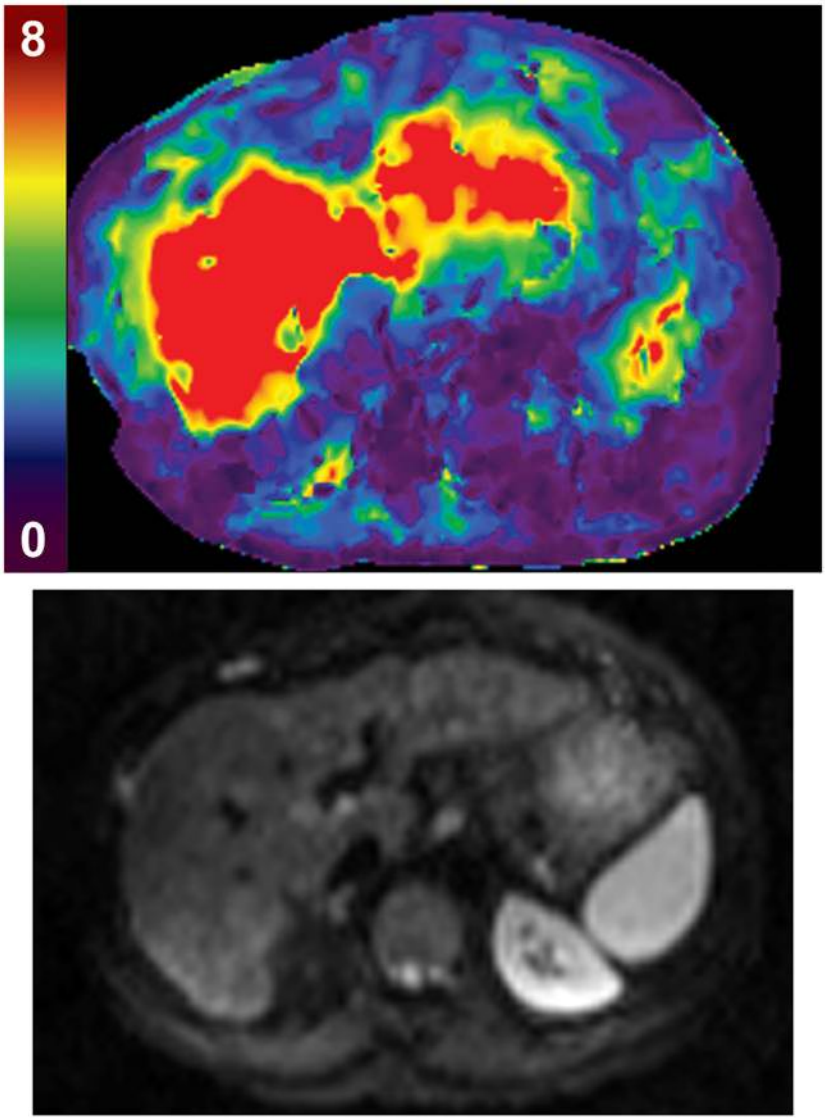

Fig. 4.

57-year-old man with history of chronic hepatitis C combined with alcohol abuse. Stage 4 hepatic fibrosis and grade 1 necroinflammatory activity are observed by histopathologic analysis following liver biopsy.

A, MR elastogram shows shear stiffness value on MRE of 11.2kPa.

B, DWI with b50 sec/mm^2 image had calculated ADC value of 0.90×10^{-3}mm^2/sec.

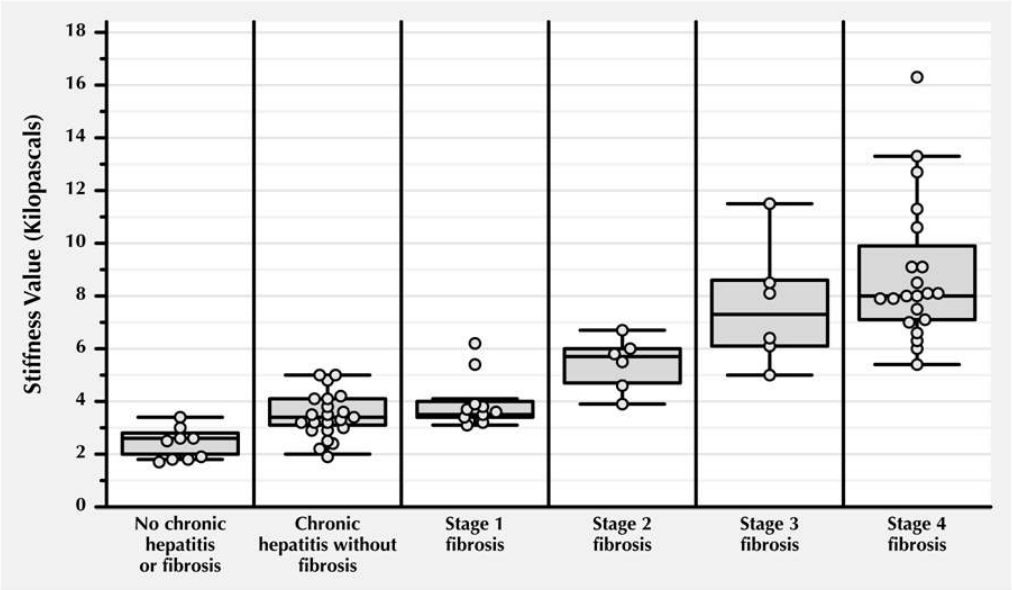

Fig. 5.

Box plot shows shear stiffness values of various stages of fibrosis. Individual data are presented as circles. The horizontal line through each box represents median value and box represents data from the 25th to the 75th percentile (middle 50% of observations). The whiskers represent data from the minimum to the maximum excluding far out values which are displayed as separate circles (Kruskal-Wallis H test and Mann-Whitney U test).

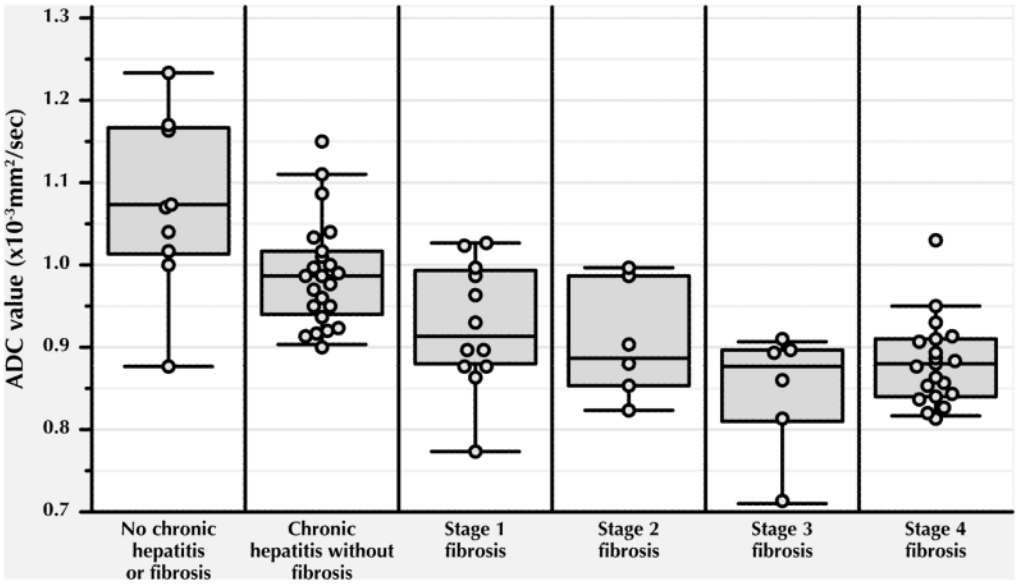

Fig. 6.

Box plot shows ADC value of various stages of fibrosis. Individual data are presented as circles. The horizontal line through each box represents median value and box represents data from the 25th to the 75th percentile (middle 50% of observations). The whiskers represent data from the minimum to the maximum excluding far out values which are displayed as separate circles (Kruskal-Wallis H test and Mann-Whitney U test).

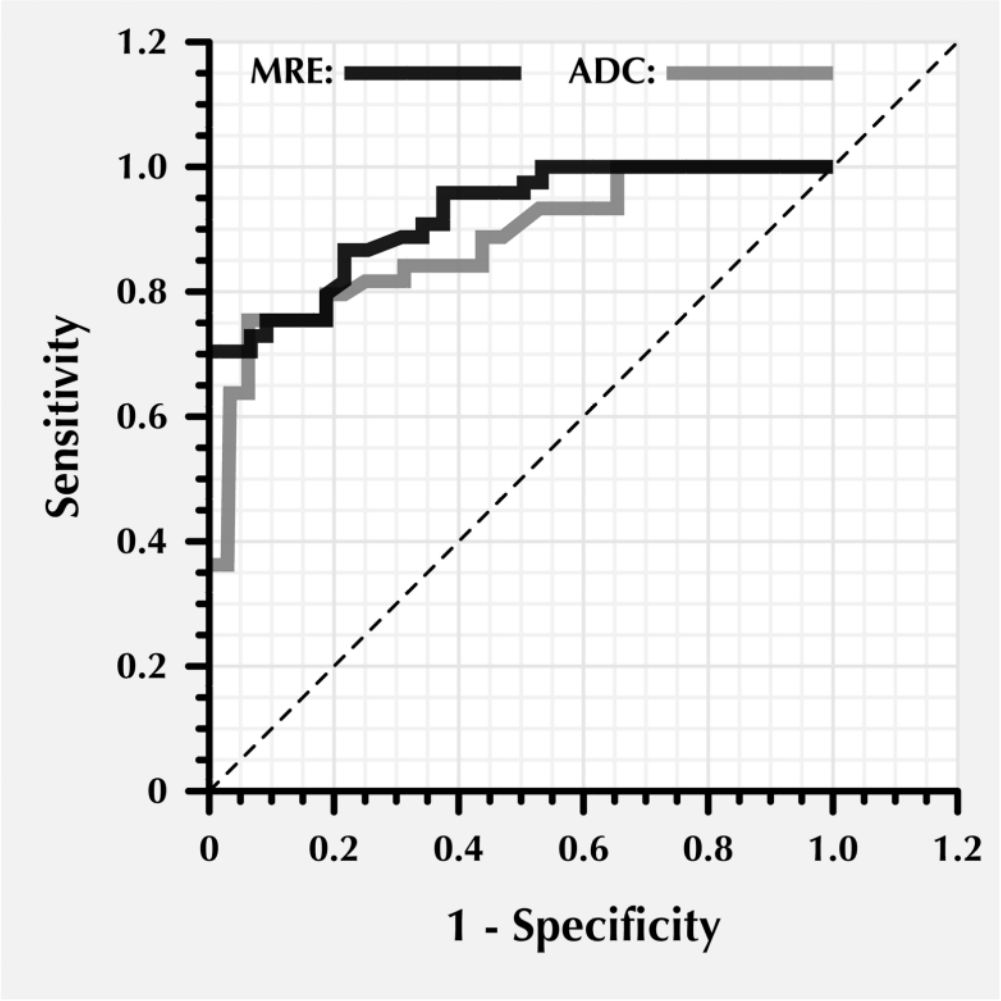

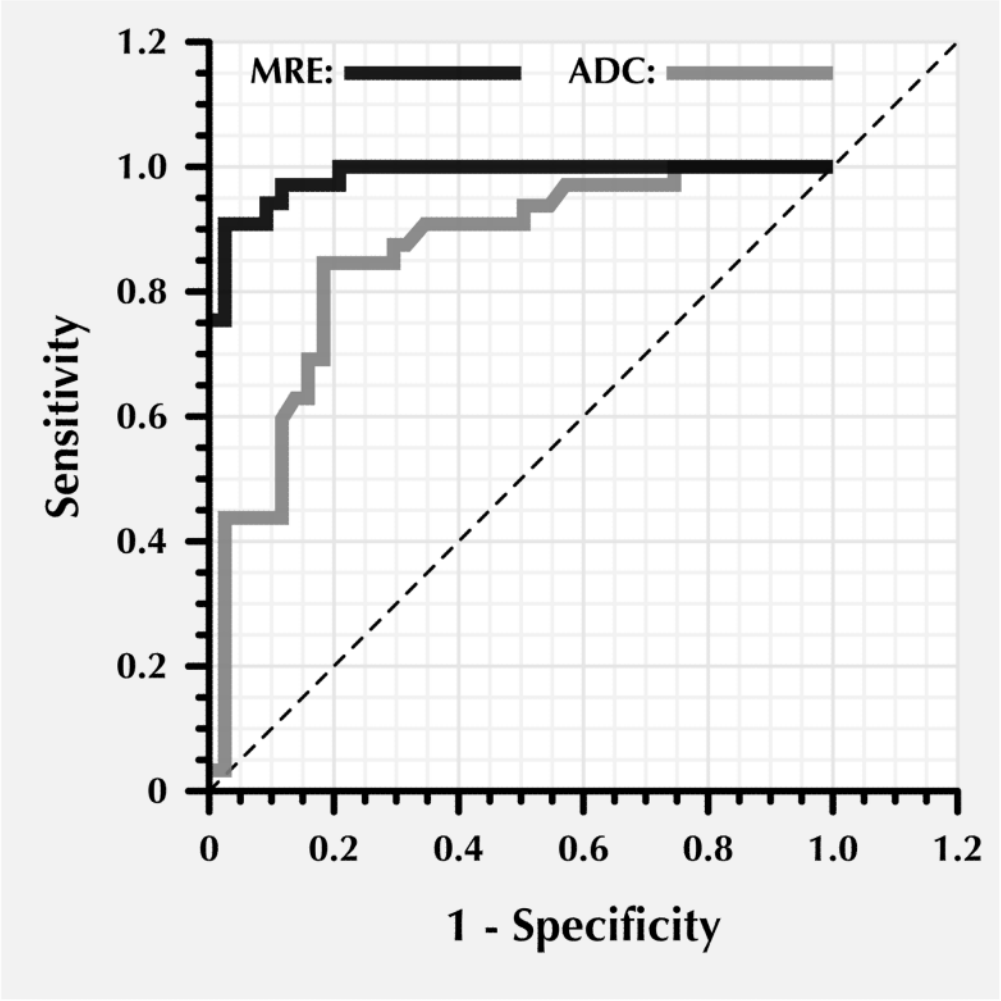

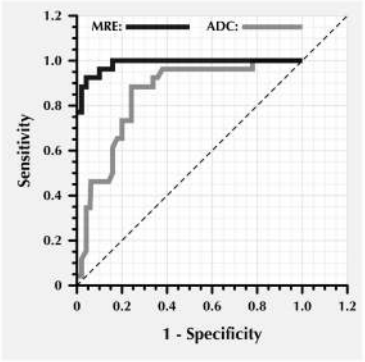

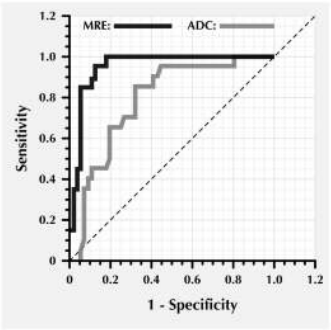

Fig. 7.

Receiver operator characteristic curves (ROC) analysis of MRE and DWI in distinguishing each stage of hepatic fibrosis

A, ROC analysis for MRE and DWI to distinguish liver tissue with no fibrosis from tissues with fibrosis stage 1 or greater (F1-4). The AUC for MRE is 0.92 (95% CI, 0.84 to 0.97) and for DWI is 0.88 (95% CI, 0.78 to 0.94). The difference in AUC is 0.04 (95% CI, -0.06 to 0.14) (*P*=0.398).

B, ROC analysis for MRE and DWI to distinguish liver tissue with no to mild fibrosis (F0-1) from moderate fibrosis to cirrhosis (F2-4). The AUC for MRE is 0.98 (95% CI, 0.92 to 1.00) and for DWI is 0.86 (95% CI, 0.76 to 0.93). The difference in AUC is 0.12 (95% CI, 0.04 to 0.22) (*P*=0.003).

C, Receiver operator characteristic curves for MRE and DWI to distinguish liver tissue with no to moderate fibrosis (F0-2) from advanced fibrosis to cirrhosis (F3-4). The AUC for MRE is 0.99 (95% CI, 0.93 to 1.00) and for DWI is 0.84 (95% CI, 0.74 to 0.92). The difference in AUC is 0.15 (95% CI, 0.06 to 0.23) (*P*=0.001).

D, Receiver operator characteristic curves for MRE and DWI to distinguish liver tissue with no to moderate fibrosis (F0-3) from advanced fibrosis to cirrhosis (F4). The AUC for MRE is 0.95 (95% CI, 0.87 to 0.99) and for DWI is 0.78 (95% CI, 0.68 to 0.87). The difference in AUC is 0.17 (95% CI, 0.06 to 0.27) (*P*=0.001).

Table 1

Distribution of various stages of fibrosis and grades of necroinflammatory activity

	NECROINFLAMMATORY ACTIVITY				
	No (A0)	**Mild (A1)**	**Moderate (A2)**	**Severe (A3)**	**Total**
No fibrosis (F0)	9	22	1	0	32
Mild fibrosis (F1)	0	9	2	1	12
Moderate fibrosis (F2)	0	3	3	0	6
Advanced fibrosis (F3)	0	0	2	4	6
Cirrhosis (F4)	0	10	10	0	20
Total	9	44	18	5	76

Table 2

Stiffness values and ADC values of healthy volunteers on two separate examinations

	Stiffness values (kPa Mean ± SD)		ADC values ($\times 10^{-3}$mm^2/sec Mean ± SD)	
	First	Second	First	Second
1	2.31±0.51	2.44±0.45	1.17±0.11	1.15±0.12
2	2.14±0.17	2.05±0.43	1.17±0.09	1.07±0.09
3	2.32±0.10	2.51±0.31	1.13±0.20	1.22±0.04
4	1.96±0.43	2.26±0.32	1.25±0.12	1.22±0.14
5	2.31±0.29	2.06±0.35	1.18±0.13	1.17±0.14

Table 3

Comparison of shear stiffness and ADC values of liver parenchyma with various stages of severity of fibrosis

	Stiffness value (kPa)	ADC value ($\times 10^{-3} mm^2/sec$)
	Median; interquartile range	**Median interquartile range**
F0	3.16; 2.62 to 3.58	1.00; 0.95 to 1.06
F1	3.50; 3.42 to 3.90	0.91; 0.88 to 0.99*
F2	5.68; 4.65 to 5.97†	0.89; 0.85 to 0.99*
F3	6.79; 6.10 to 8.56‡	0.88; 0.81 to 0.90*
F4	8.06; 7.07 to 9.91‡	0.88; 0.84 to 0.91*

*different from F0; $P<0.05$

†different from F0, F1; $P<0.05$

‡different F0, F1, F2; $P<0.05$

Table 4

Comparison of overall predictive power of MRE and DWI in predicting and staging fibrosis

	F0/ F1-4 (95% CI)	F0-1/ F2-3-4 (95% CI)	F0-1-2/ F3-4 (95% CI)	F0-1-2-3/ F4 (95% CI)
Stiffness value (kPa)				
Cut-off value	5.02	5.37	5.97	5.97
Sensitivity (%)	72 (56 to 85)	91 (75 to 98)	92 (75 to 99)	95 (75 to 100)
Specificity (%)	100 (88 to 100)	97 (87 to 100)	95 (86 to 100)	87 (75 to 94)
PPV (%)	100 (88 to 100)	97 (83 to 100)	92 (74 to 99)	73 (55 to 88)
NPV (%)	72 (56 to 85)	93 (81 to 99)	96 (86 to 100)	98 (89 to 100)
ADC value ($\times 10^{-3} mm^2/sec$)				
Cut-off value	0.91	0.91	0.91	0.91
Sensitivity (%)	75 (60 to 87)	84 (67 to 95)	88 (70 to 87)	85 (62 to 97)
Specificity (%)	94 (79 to 99)	82 (67 to 92)	76 (51 to 77)	68 (54 to 79)
PPV (%)	94 (81 to 99)	77 (60 to 90)	66 (48 to 81)	49 (31 to 66)
NPV (%)	73 (57 to 86)	87 (74 to 96)	93 (80 to 99)	93 (80 to 99)